

# Molecular Dynamics of a Polyaniline/ $\beta$ -Cyclodextrin Complex Investigated by $^{13}\text{C}$ Solid-State NMR

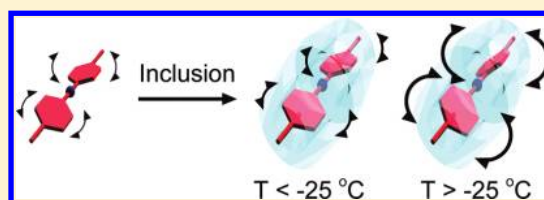
Yuichi Hasegawa,<sup>†</sup> Yoshio Inoue,<sup>†</sup> Kenzo Deguchi,<sup>‡</sup> Shinobu Ohki,<sup>‡</sup> Masataka Tansho,<sup>‡</sup> Tadashi Shimizu,<sup>‡</sup> and Koji Yazawa<sup>\*,†,§</sup>

<sup>†</sup>Department of Biomolecular Engineering, Tokyo Institute of Technology, 4259 Nagatsuta-cho, Midori-ku, Yokohama, Kanagawa 226-8501, Japan

<sup>‡</sup>National Institute for Materials Science, 3-13 Sakura, Tsukuba, Ibaraki 305-0003, Japan

<sup>§</sup>Department of Biotechnology, Tokyo University of Agriculture and Technology, 2-24-16 Naka-cho, Koganei, Tokyo 184-8588, Japan

**ABSTRACT:** The molecular dynamics of a polyaniline/ $\beta$ -cyclodextrin inclusion complex (PANI/ $\beta$ -CD IC) and its relation with optical properties were investigated using high-resolution solid-state  $^{13}\text{C}$  nuclear magnetic resonance (NMR) and optical absorption spectroscopies. UV–vis measurements revealed a  $\pi$ – $\pi^*$  absorption peak of a PANI film that had a 10 nm blue-shift by inclusion of  $\beta$ -CD, indicating that  $\pi$ -conjugation of PANI was shortened in the IC. Temperature dependent analysis of  $^{13}\text{C}$  NMR spectra and spin–lattice relaxation times ( $T_{1\text{C}}$ ) revealed that the inclusion induced acceleration of the twisting motion of the PANI chain. Moreover, two twisting motions attributed to different torsional angle modes were observed following Arrhenius plots of  $T_{1\text{C}}$  measurements, and the twisting frequency and angle increased above  $-25^\circ\text{C}$ . These results suggest that the  $\beta$ -CD inclusion weakens the intermolecular  $\pi$ – $\pi$  interaction and enhances the accompanying twisting motion, consequently leading to a blue-shift of UV–vis absorption.



## 1. INTRODUCTION

The  $\pi$ -conjugated polymers are candidate materials for electronic and optoelectronic devices<sup>1</sup> because they have carrier mobility and desirable optical properties such as visible absorption, emission, and a nonlinear optical effect. Among these materials, polyaniline (PANI) is a promising conducting polymer for many applications such as pH sensors<sup>2</sup> and batteries<sup>3</sup> because of its environmental stability, and the possibility of conductivity control by redox.

The electronic and optical properties of  $\pi$ -conjugated polymers are known to be influenced by molecular dynamics other than static structure, such as aggregation structure, planarity of chain, and intermolecular  $\pi$ – $\pi$  stacking. The thermochromism phenomenon is a representative example of the influence of molecular dynamics on optical properties. The twisting motion of conjugated chains is thermally excited and shortens the conjugation length. The high-resolution solid-state nuclear magnetic resonance (NMR) technique, particularly  $^{13}\text{C}$  spin–lattice relaxation time ( $T_{1\text{C}}$ ) measurement, is a hopeful method to analyze the static and dynamic structure of polymers. For a conjugated polymer, poly(5,7-dodecadiyne-1,12-diol bis-(ethylurethane)), a blue-shift of the absorption wavelength and decrease of  $^{13}\text{C}$  spin–lattice relaxation time ( $T_{1\text{C}}$ ) occur simultaneously with increasing temperature.<sup>4</sup> This implied that polymer motion which was accelerated with increased temperature shortened the  $\pi$ -conjugation length and resulted in the blue-shift of the absorption maximum. We also previously reported that aliphatic side-group motion of poly(3-hexylthiophene) in the crystalline state weakened their intermolecular

$\pi$ – $\pi$  interaction, and subsequent thiophene twisting motion collapsed not only intermolecular but also intrachain  $\pi$ -conjugation, and consequently the blue-shift of the absorption peaks originated from both the interchain and intramolecular exciton.<sup>5</sup> Moreover, carrier mobility is suppressed above the main chain twisting transition temperature, suggesting the effect of twisting motion on interference of effective conjugation.<sup>6</sup> Thus, the dynamic structure of the  $\pi$ -conjugated polymer has a crucial effect on  $\pi$ -conjugation length. However, it is still unknown whether the main cause of the blue-shift in absorption wavelength is due to intrachain twisting motion itself or a weakened intermolecular  $\pi$ – $\pi$  interaction caused by the twisting motion. Therefore, investigation of the dynamic structure of the  $\pi$ -conjugated polymer system without the  $\pi$ – $\pi$  interaction is needed to distinguish the above causes.

A representative method to isolate polymer chains in a bulk system is to make an inclusion complex (IC) in which a single polymer chain penetrates some cyclic molecules and forms a necklace-like structure. Using the IC structure, the intrinsic properties of a polymer without the effect of various intermolecular interactions would be obtained. Especially in the case of a  $\pi$ -conjugated polymer, we are able to remove the complicated  $\pi$ – $\pi$  stacking effect, which has a marked influence on electronic and optoelectronic properties of a conducting polymer.

Received: August 4, 2011

Revised: January 10, 2012

Published: January 10, 2012



Harada et al. prepared an IC for the first time in which polyethyleneglycol penetrates many cyclic  $\alpha$ -cyclodextrins (CDs) in a manner resembling a necklace.<sup>7</sup> CDs are kinds of cyclic molecules, consisting of six, seven, or eight glucoses and are called  $\alpha$ -,  $\beta$ -, and  $\gamma$ -CD, respectively. They are able to include low-molecular substances and high-molecular polymers in their cavity and form ICs. So far, various ICs with macromolecular substances have been reported.<sup>8–10</sup>

The first report of an IC with  $\pi$ -conjugated polymers was presented by Yoshida et al.<sup>11</sup> They prepared an IC consisting of conducting PANI and  $\beta$ -CD. The conformational change in PANI from a coil-like to rod-like structure occurred by forming the IC with  $\beta$ -CD. In this structure,  $\beta$ -CD protects PANI from chemical attack by iodine-like molecules.<sup>12</sup> It is also predicted that  $\beta$ -CD prevents electron transfer among polymer chains. Therefore, the IC is expected to show one-dimensional conduction along a molecular chain, leading to application in molecular devices such as molecular wires. Several studies regarding preparation of IC comprising PANI and  $\beta$ -CD have been reported.<sup>13–16</sup> According to Belosludov's calculations, aniline rings of PANI in IC are predicted to line up planarly and form a long conjugation length, resulting in high conductivity<sup>17</sup> in comparison to a single PANI chain. Its structure is thought to have no intermolecular  $\pi$ - $\pi$  stacking effect among PANI chains and to show a property comparable to one molecule that is not affected by interactions. Therefore, the molecular dynamics of a  $\pi$ -conjugated polymer in the IC structure has attracted much attention not only for application in various devices but also in regard to basic research.

The molecular dynamics of inclusion complexes consisting of aliphatic polymers and CDs have been studied.<sup>18–20</sup> Lu et al. reported the molecular dynamics of semicrystalline polycaprolactone (PCL) in  $\alpha$ - and  $\gamma$ -CD using the <sup>13</sup>C NMR spin-lattice relaxation time method.  $\alpha$ - and  $\gamma$ -CD can include a single PCL and two that are parallel or side-by-side, respectively.<sup>18</sup> PCL in CDs have a 500–1000 times shorter  $T_{1C}$  than their bulk state regardless of CD cavity size. This suggests that the MHz order motion like torsion around the molecular axis was facilitated because tight packing among PCL chains was removed by inclusion of CDs.

On the other hand, the molecular dynamics of a CD/ $\pi$ -conjugated polymer system, especially in regard to functions, such as carrier mobility and optical properties have not been investigated.

In this study, we report the molecular dynamics of PANI without an intermolecular  $\pi$ - $\pi$  interaction by an inclusion complex with  $\beta$ -CD, possessing a chemical structure, as shown in Figure 1, using high-resolution solid-state <sup>13</sup>C nuclear magnetic

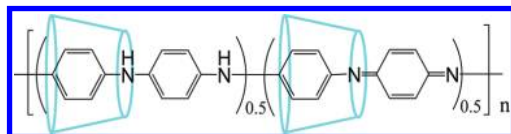


**Figure 1.** Chemical structure of the polyaniline/ $\beta$ -CD inclusion complex.

resonance spectroscopy (NMR) and discuss how a reduction of  $\pi$ - $\pi$  stacking influences the molecular motion of PANI and resulting optical properties.

## 2. EXPERIMENTAL METHODS

*N*-Phenyl-1,4-phenylenediamine (PPD) and ammonium persulfate (APS) were purchased from Tokyo Chemical Industry,

and  $\beta$ -CD was purchased from Wako Pure Chemical Industries. All compounds were used without further purification. PANI/ $\beta$ -CD IC was synthesized by referring to the literature.<sup>13</sup> A 0.3 g portion of PPD and 3.0 g of  $\beta$ -CD were dissolved in 50 mL of ethanol and 400 mL of water, respectively. The two solutions were mixed and evaporated until reaching a volume of 250 mL. Brown powder was then collected by freeze dehydration. Free PPD was washed with acetone, and PPD/ $\beta$ -CD IC was eventually collected.

A 2.8 g portion of PPD/ $\beta$ -CD IC was dissolved in 175 mL of water, and 0.5 g of APS was dissolved in another 50 mL of water. The APS solution was added to the PPD/ $\beta$ -CD IC solution dropwise at 0 °C for 5 h and stirred for 1 day. After the reaction, the solution was centrifuged and washed with pure water to remove pure  $\beta$ -CD, and then PANI/ $\beta$ -CD IC was obtained under reduced pressure. After stirring, the aqueous solution of PANI/ $\beta$ -CD IC at 80 °C for 5 h, neat PANI was obtained by centrifugation and dried under reduced pressure.

<sup>1</sup>H NMR measurements were performed using 600 MHz Bruker AVANCE as solution in DMSO-*d*<sub>6</sub> to estimate the stoichiometric ratio of PANI and  $\beta$ -CD.

Mass spectra of the obtained PANI in the IC were recorded using Shimadzu Biotech Axima CFR plus matrix assisted laser desorption ionization time-of-flight mass spectrometry (MALDI-TOFMS) by the solventless method. The measurement was carried out using the reflector mode. The samples of neat PANI were prepared in a manner similar to that previously reported.<sup>21</sup> Neat PANI and matrix (dithranol) were mixed in a mortar with a pestle in order to reduce the size of the PANI particles. A molar ratio of analyte to matrix of 1:50 was used.

UV-vis spectra in the solid state were measured using a spectrophotometer (V-550, JASCO). All of the samples were cast on a polymethylmethacrylate (PMMA) plate from the *N*-methylpyrrolidone solution and dried under reduced pressure.

The wide-angle X-ray diffraction patterns were recorded at 40 kV and 200 mA using nickel-filtered Cu K $\alpha$  radiation on a RINT 2500 X-ray diffractometer (Rigaku) at a scanning speed rate of 1°/min.

Variable temperature <sup>13</sup>C cross-polarization and magic-angle spinning (CPMAS),<sup>22</sup> spin-lattice relaxation time ( $T_{1C}$ ), and that in a rotating system ( $T_{1\rho C}$ ) were utilized to obtain measurements using a NMR spectrometer (JNM-ECA-500; JEOL) equipped with a 4 mm MAS probehead, operating at 500 MHz for <sup>1</sup>H and 125.8 MHz for <sup>13</sup>C. For CPMAS and relaxation measurements, experimental conditions were set up with a 90° pulse length of 3.1  $\mu$ s, contact time of 1 ms for IC and 0.3 ms for neat PANI, a recycle delay of 1 s, and a MAS rate of 10 kHz. The <sup>13</sup>C chemical shifts were referenced externally to the methyl carbon resonance of hexamethylbenzene at 17.4 ppm. We used the Torchia method<sup>23</sup> for  $T_{1C}$  measurements.

## 3. RESULTS AND DISCUSSION

First, we performed a <sup>1</sup>H NMR measurement in DMSO-*d*<sub>6</sub> to calculate the consistency of PANI and  $\beta$ -CD in the product. The stoichiometry of PANI/ $\beta$ -CD IC was determined by the rate of integral intensities of the PANI signal (14 H, 6.5–7.5 ppm) to that of the H<sub>1</sub> signal (7 H, 4.7 ppm) of  $\beta$ -CD, and the obtained result was 4.5: 1 (aniline unit:  $\beta$ -CD).

Polymerization of PANI was confirmed from characteristic peaks of high-molecular weight PANI in an FTIR spectrum;<sup>24</sup> C–N stretching of secondary aromatic amine at 1315 cm<sup>–1</sup>, C=C stretching of benzenoid rings at 1502 cm<sup>–1</sup>, and C=N

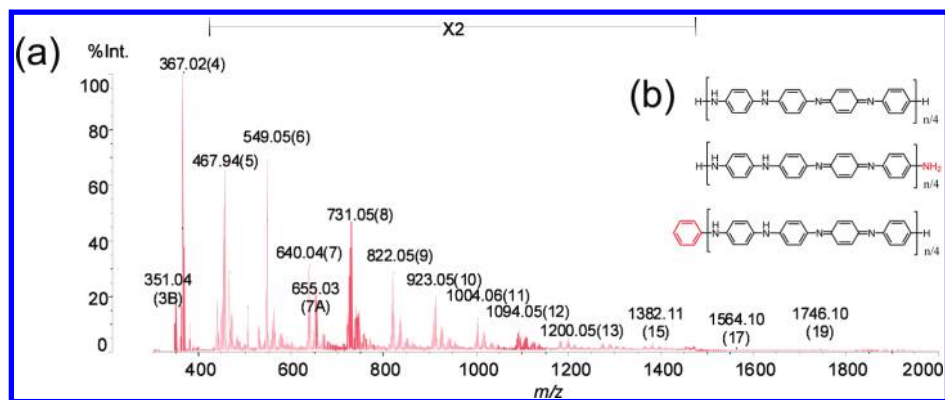


**Figure 2.** (a) A solventless MALDI-TOFMS spectrum of neat PANI in a 1:50 molar ratio with dithranol. (b) Structures for the three different types of end groups on PANI. The first is terminated by a phenyl group on both ends, the second contains equal numbers of a phenyl and nitrogen-containing group, and the third contains an additional nitrogen-containing group.

stretching of quinoid rings at  $1572\text{ cm}^{-1}$ , which exist in PANI and not PPD.

The molecular weight of PANI in the obtained IC was investigated by MALDI-TOFMS measurement. A solventless MALDI-TOFMS spectrum of neat PANI in a 1:50 molar ratio with dithranol is shown in Figure 2a. We observed signals of 4–19 mers of PANI. The peak derived from tetramer was strongest, and the intensity decreased with increasing molecular weight. Here, we should consider that ionization of the sample might be depressed with the higher molecular weight. Thus, there is no guarantee that the signal intensity directly represents the amount. In addition, some amount of PANI with an even number of aniline was observed although PANI with an odd number should be synthesized theoretically because the dimer, PPD, was used as the smallest unit for the synthesis. This implies that the samples were decomposed in the process of ionization such as laser radiation. The fact that three peaks appear in each of the oligomers supports the decomposition of PANI as previously described.<sup>21</sup> PANI should mainly contain equal numbers of phenyl and nitrogen-containing terminal groups. However, the appearance of the other two peaks indicates the presence of PANI with phenyl or nitrogen-containing terminal groups on both ends, as described in Figure 2b. Regardless, we can conclude from the MALDI-TOF measurement that at least 4–19 mers of PANI were synthesized.

Next, we confirmed the inclusion structure of PANI/ $\beta$ -CD IC by WAXD patterns. Figure 3a shows WAXD spectra for pure  $\beta$ -CD, PANI/ $\beta$ -CD IC, and neat PANI.  $\beta$ -CD is known to form two crystal structures: a cage and channel structure<sup>25</sup> as described in Figure 3b. While pure  $\beta$ -CD tends to form the cage structure, IC with polymers and CDs form the channel structure. The two structures can be distinguished by WAXD patterns. The diffraction peaks of  $11.8^\circ$  and  $17.7^\circ$  were observed for PANI/ $\beta$ -CD IC, as shown in Figure 3a. These were characteristic peaks of a channel structure of  $\beta$ -CD,<sup>8</sup> which correspond to  $d$ -spaces of 0.76 and 0.50 nm, respectively, as shown in Figure 3c, and indicate the formation of an IC structure.

Figure 4 shows UV–vis spectra for PANI/ $\beta$ -CD IC and neat PANI in an NMP solution and a cast sample on a PMMA plate. All of the samples showed two absorption peaks. The shorter wavelength absorption peak is attributed to a  $\pi$ – $\pi^*$  transition and the longer wavelength to an  $n$ – $\pi^*$  transition.<sup>26</sup> According to the literature, we can estimate the polymerization degree of PANI by finding the peak position in the NMP solution.

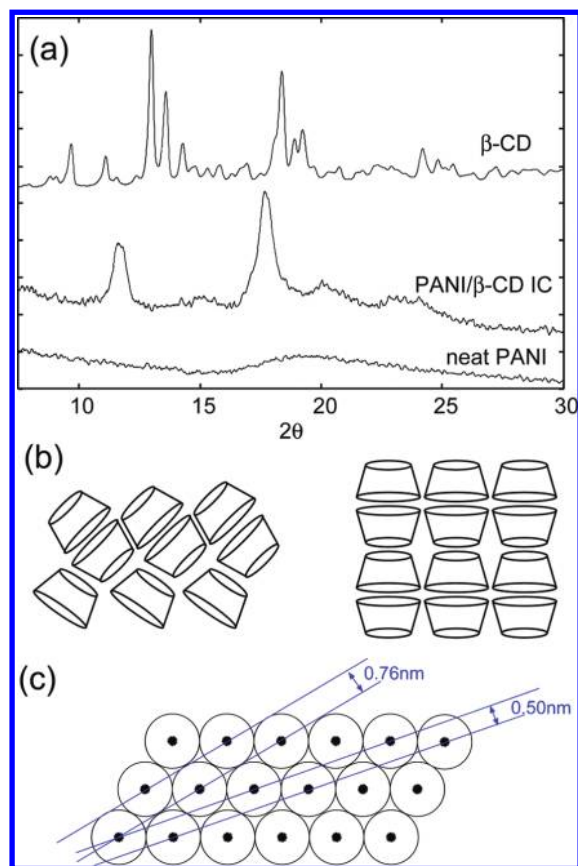


**Figure 3.** (a) WAXD patterns for  $\beta$ -CD, PANI/ $\beta$ -CD IC, and neat PANI. (b) Schematic depiction of cage (left) and channel (right) structures of CDs. (c) Sketch of an IC structure with expected  $d$ -spaces corresponding to the observed peaks in the WAXD spectrum.

The peak at 603 nm of the  $n$ – $\pi^*$  transition for neat PANI could be estimated at 4–16 mer on average because it is a longer wavelength than 590 nm of the aniline tetramer and shorter than 610 nm of the 16 mer.<sup>27</sup> This is almost consistent with the result of MALDI-TOFMS.

A red-shift of the  $n$ – $\pi^*$  transition peak of PANI by  $\beta$ -CD inclusion has been reported.<sup>13</sup> The PANI chain restricted by  $\beta$ -CD formed a more planar structure, resulting in stabilization of  $\pi$ -conjugation. However, a red-shift of PANI absorption by  $\beta$ -CD inclusion was not observed in our research. There are some possible reasons for this result. In this research, the



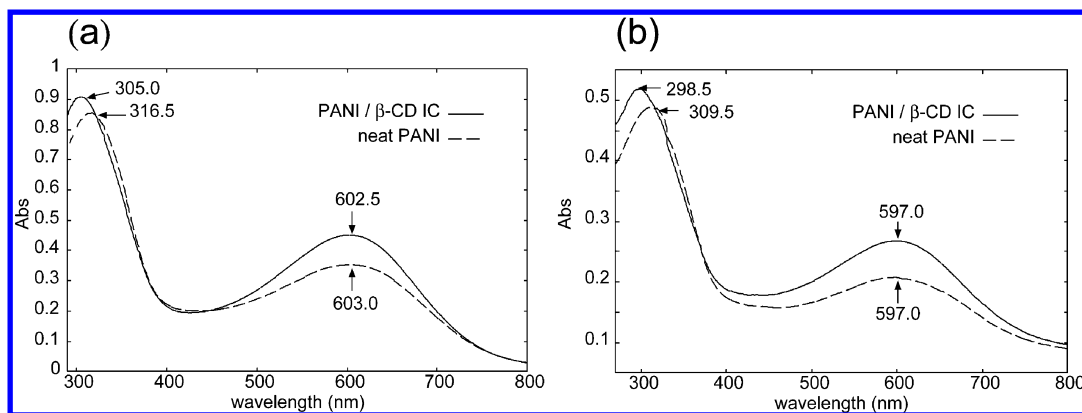


Figure 4. UV-vis spectra for (a) PANI/ $\beta$ -CD IC and neat PANI in NMP solution and (b) their films on PMMA substrates.

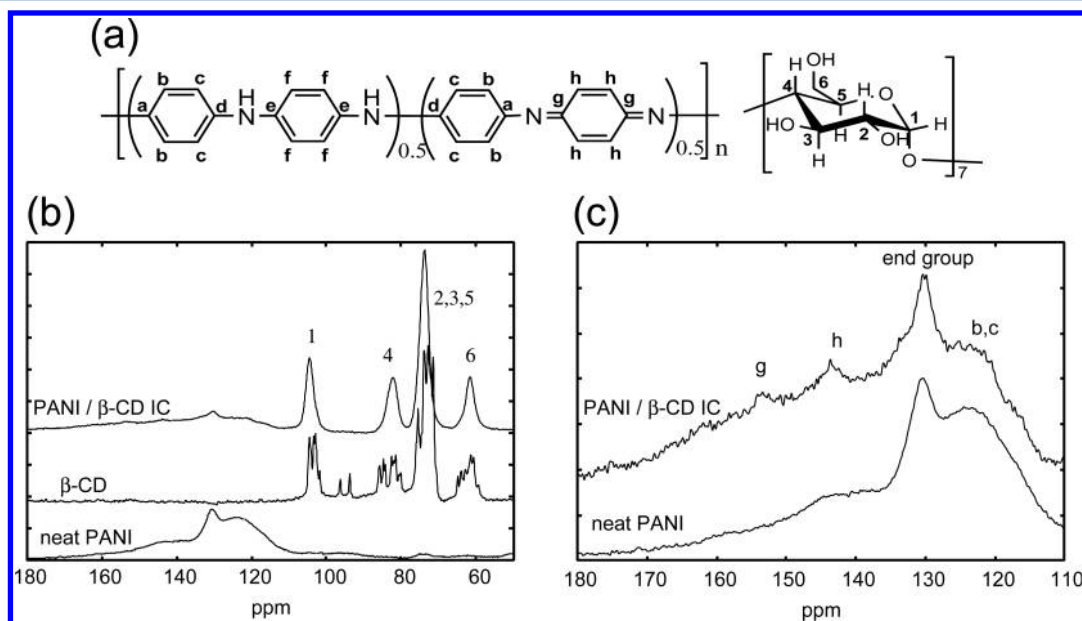


Figure 5.  $^{13}\text{C}$  CPMAS NMR spectra for PANI,  $\beta$ -CD, and PANI/ $\beta$ -CD IC: (a) the chemical structure of PANI and  $\beta$ -CD, (b) the whole range of spectra, and (c) the extended spectra for the region of PANI carbons.

stoichiometrical ratio of  $\beta$ -CD for PANI/ $\beta$ -CD IC was small and the molecular weight of PANI is low. As a result, the planar effect of  $\pi$ -conjugation is expected to be small. Another reason is the fact that we measured a solid state sample, in addition to the NMP solution as reported in the literature. In the solid state, a planar effect of the PANI chain and destabilization of the  $\pi$ - $\pi$  interaction by  $\beta$ -CD inclusion would occur. In addition, the  $\pi$ - $\pi^*$  transition peak brought a blue-shift of about 10 nm by inclusion. This suggests that in the solid state the conjugation length of PANI is shortened by  $\beta$ -CD because of interruption of  $\pi$ - $\pi$  stacking.

To elucidate the inclusion effect on the dynamic structure of PANI, we performed  $^{13}\text{C}$  solid state NMR measurements. First, we performed  $^{13}\text{C}$  CPMAS measurements and derived spectra are shown in Figure 5. Peaks corresponding to  $\beta$ -CD and PANI carbons appeared in the ranges 55–105 and 110–170 ppm, respectively. The assignments of each carbon were made with reference to the literature.<sup>28,29</sup> While pure  $\beta$ -CD showed split peaks,  $\beta$ -CD IC showed broad signals. Similar results were observed in other CD/polymer IC systems such as  $\alpha$ -CD/poly(ethylene glycol),<sup>30</sup>  $\beta$ -CD/poly(propylene glycol),<sup>8</sup> and  $\beta$ -CD/poly(neopentyl glycol).<sup>31</sup>  $\beta$ -CD without any guest

molecules has a less symmetrical conformation, resulting in the split peaks. On the other hand, the peaks of CD in IC are broadened because the electron environment of each carbon atom of CD becomes equal by inclusion. The fact that our result shows a similar tendency with other CD/polymer systems is more evidence of IC formation.

Broad PANI component peaks of PANI/ $\beta$ -CD IC and neat PANI were observed with the same shape regardless of inclusion. A peak corresponding to the outside of the benzenoid ring (b and c) and outside of the quinoid ring (h) appeared around 125 and 144 ppm, respectively. The strongest peak was observed at 130 ppm. This peak did not exist in the case of high-molecular PANI.<sup>29</sup> On the other hand, the meta-position of the PPD phenyl end appeared at 129.1 ppm of  $^{13}\text{C}$  NMR solution spectra dissolved in  $\text{CDCl}_3$ . Therefore, we could assign this peak derived from the meta-position of the PANI end group and call it the “end group”. We also call the peak around 125 ppm (b, c) “benzenoid”.

We measured the  $^{13}\text{C}$  spin-lattice relaxation time ( $T_{1\rho\text{C}}$ ) and that in the rotating frames ( $T_{1\rho\text{C}}$ ) for the end group and benzenoid peak in the temperature range  $-100$  to  $90^\circ\text{C}$  to investigate the effect of inclusion on molecular dynamics.

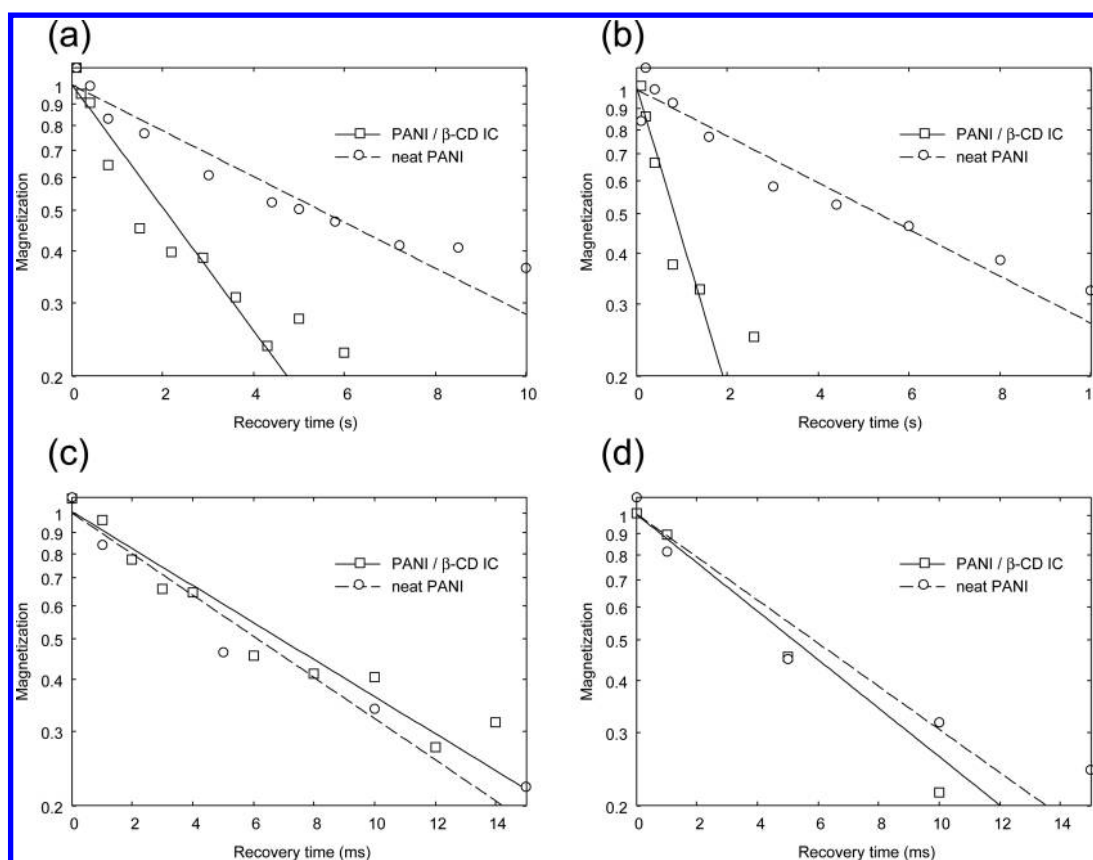


**Figure 6.**  $^{13}\text{C}$  spin–lattice relaxation curves for the end group peak of PANI and PANI/ $\beta$ -CD IC measured at (a) 25 °C and (b) 90 °C and  $^{13}\text{C}$  spin–lattice relaxation curves in the rotating frames measured at (c) 25 °C and (d) 90 °C.

Relaxation curves for the end group peak at 25 and 90 °C are shown in Figure 6.

For the end group peak and benzenoid peak, each  $T_{1\text{C}}$  value was obtained using a single exponential fitting curve:

$$M_z(t) = M_z(0) \exp\left(-\frac{t}{T_{1\text{C}}}\right) \quad (1)$$

where  $M_z$  is the magnetization along the magnetic field.

The decay of magnetization of a compound in a glassy state generally obeys the stretched exponential fitting curve, given as  $M_z(t) = \exp(-R_1 t)^\beta$ , where  $\beta$  is a stretched index. In fact, we can observe a slight deviation of the observed decay from the single exponential. In practice, however, temperature dependence of  $\beta$  cannot be described as a simple formula in the polymer system as described in our previous report.<sup>32</sup> In addition, it is hard to provide a physical meaning to  $\beta$  in the IC system. Thus, we performed the single exponential analysis. It is thought that an average of T1 values and its relative temperature dependence obtained by the analysis using a single exponential fit is meaningful, although this analysis cannot absolutely describe an accurate T1 relaxation. Obtained  $T_{1\text{C}}$  values in neat PANI and PANI/ $\beta$ -CD IC are shown in Table 1a. The  $T_{1\text{C}}$  value is sensitive to molecular dynamics around the Larmor frequency at 125 MHz. Translation and twisting are possible motions corresponding to this frequency. However, the possibility of translational motion would be very small because all measurements were performed under a glass transition temperature for neat PANI, 220 °C,<sup>33</sup> and PANI/ $\beta$ -CD IC forms a channel-type crystalline structure in the temperature range as observed in the WAXD measurement. Therefore,

**Table 1.** (a)  $^{13}\text{C}$  Spin–Lattice Relaxation Times ( $T_{1\text{C}}$ , s) and (b) Spin–Lattice Relaxation Times in the Rotating Frame ( $T_{1\rho\text{C}}$ , ms) for the PANI Component Peak in the PANI/ $\beta$ -CD IC and Neat PANI

$T$ (°C)	end group		benzenoid	
	PANI	IC	PANI	IC
(a) $T_{1\text{C}}$ (s)				
−100	15.2 ± 1.8	10.2 ± 1.5	18.7 ± 4.1	15.1 ± 3.7
25	7.9 ± 0.8	3.0 ± 0.4	6.7 ± 0.9	3.3 ± 0.5
90	7.6 ± 1.0	1.1 ± 0.3	5.1 ± 0.6	2.1 ± 1.3
(b) $T_{1\rho\text{C}}$ (ms)				
−100	17.2 ± 1.8	16.7 ± 1.7	15.9 ± 2.1	17.0 ± 1.9
25	8.2 ± 1.4	9.8 ± 0.8	7.3 ± 1.0	7.6 ± 0.7
90	8.0 ± 1.6	7.4 ± 0.9	9.2 ± 1.7	6.8 ± 1.1

$T_{1\text{C}}$  values likely reflect the twisting motion around the molecular axis. On the other hand, the  $T_{1\rho\text{C}}$  value is influenced by molecular dynamics around the spin lock frequency of 80 kHz and corresponds to the molecular dynamics all over the chain.

$T_{1\text{C}}$  values of the end group and benzenoid components of PANI/ $\beta$ -CD IC were shorter than those of neat PANI at all temperatures. For example, their values at 25 °C were, respectively, 2.6 and 2.2 times shorter than that of neat PANI. This suggests that  $\beta$ -CD inclusion accelerates twisting motion around the PANI axis.

Inclusion generally accelerates molecular dynamics when an included polymer is a crystalline polymer such as polycaprolactone (PCL) because it removes tight packing among polymer chains.<sup>18</sup> Interestingly, twisting motion of the PANI chain

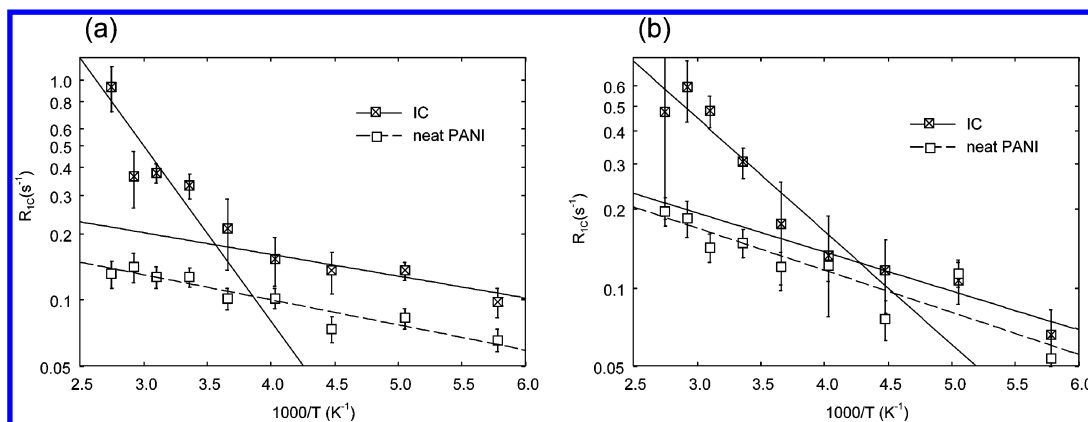


Figure 7. Arrhenius plots of  $T_{1C}$  for the (a) end group of PANI and PANI/ $\beta$ -CD IC and (b) benzenoid component of PANI and PANI/ $\beta$ -CD IC.

was promoted although pure PANI is an amorphous polymer. This result suggests that the  $\pi$ - $\pi$  stacking effect of PANI is strong enough to depress twisting motion even in an amorphous state.

Activation energy is a good indicator of the twisting angle. When the decay of magnetization obeys Debye-type relaxation in the measurement temperature, we can determine the activation energy  $E_a$  using the results of temperature-dependent  $T_{1C}$  measurement.<sup>5</sup> The spectral density function  $J(\omega_0)$  is shown with the following equation:

$$J(\omega_0) = \frac{\tau_c}{1 + \omega_0^2 \tau_c^2} \quad (2)$$

where  $\omega_0$  is the resonant frequency and  $\tau_c$  is the correlation time. In the slow-motion regime ( $\omega_0 \tau_c \gg 1$ ), the activation energy is described by the following equation:

$$R_1 \approx \frac{M_2^2}{\omega_0^2} \exp\left(-\frac{E_a}{RT}\right) \quad (3)$$

where  $R_1$  is a rate constant ( $=1/T_{1C}$ ) and  $M_2$  is the second moment of the fluctuating local field. We roughly estimated the activation energy for neat PANI and IC from the temperature dependence of  $R_1$ .

Arrhenius plots for the end group and benzenoid components of neat PANI and IC are shown in Figure 7. It is noteworthy that two activation energies were observed below and above  $-25^\circ\text{C}$  for PANI/ $\beta$ -CD IC, although neat PANI exhibited only one value over the measured temperature range for both components. Activation energies ( $E_a$ ) calculated from the Arrhenius plots are listed in Table 2.  $E_a$  values of neat PANI components and PANI/ $\beta$ -CD IC below  $-25^\circ\text{C}$  were almost the same. However, the  $E_a$  value for PANI/ $\beta$ -CD IC increased significantly above  $-25^\circ\text{C}$ , indicating that the PANI component of PANI/ $\beta$ -CD IC transfers to different phases around  $-25^\circ\text{C}$ . Since we could not confirm any transition point with DSC measurement (data not shown), this transition was presumed to have little change in specific heat. If the transition derives from acceleration of twisting motion around the molecular axis with the same torsion angle, the  $E_a$  value should decrease above the transition temperature. Thus, an increase of the  $E_a$  value above  $-25^\circ\text{C}$  by inclusion of  $\beta$ -CD conflicted with torsional acceleration by inclusion. Therefore, we predict that a change in the twisting angle of PANI occurred around this transition point. The scale of  $E_a$  values (several kJ/mol) is almost equal with  $E_a$  values in thiophene rings of

Table 2. Activation Energies ( $E_a$ , kJ/mol) for the End Group and Benzenoid Components of PANI and PANI/ $\beta$ -CD IC

	$E_a$ (kJ/mol)			
	end group		benzenoid	
	$T < -25^\circ\text{C}$	$T > -25^\circ\text{C}$	$T < -25^\circ\text{C}$	$T > -25^\circ\text{C}$
IC	$1.8 \pm 0.5$	$15.3 \pm 5.0$	$2.9 \pm 0.7$	$8.3 \pm 2.5$
neat PANI	$2.2 \pm 0.3$		$3.1 \pm 0.6$	

poly(3-hexylthiophene) (P3HT),<sup>5</sup> and  $E_a$  values commonly increased step-by-step with an increase in temperature. A proposed scheme of twisting motion is shown in Figure 8.

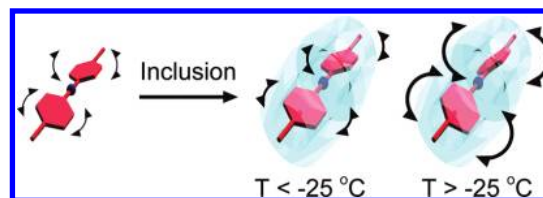


Figure 8. A proposed scheme of twisting motion.

Neat PANI and PANI/ $\beta$ -CD IC twist with the same torsional angle below  $-25^\circ\text{C}$ , although the rate of twisting motion for PANI in IC is slightly more rapid than that for neat PANI. Above  $-25^\circ\text{C}$ , PANI/ $\beta$ -CD IC changes to another phase with a wider twisting angle and rapid motion. The slightly larger activation energy of the end group than the benzenoid component implies a wider twisting angle for the end group. Unfortunately, the cause of this transition is still unclear because no transition was observed in other measurements such as DSC. Thus, further studies are needed to elucidate the cause of this transition.

At any rate, we can be fairly certain that a strong intermolecular  $\pi$ - $\pi$  interaction repressing molecular dynamics of the PANI chain was removed by inclusion.

$T_{1\rho C}$  values of the end group and benzenoid peaks in neat PANI and IC are shown in Table 1b. The  $T_{1\rho C}$  value hardly changed by  $\beta$ -CD inclusion over the measured temperature range, indicating that molecular dynamics over the whole polymer length were merely facilitated by inclusion.

These two kinds of relaxation measurements revealed that inclusion by  $\beta$ -CD did not influence the slow motion over the chain but strongly facilitated local rapid twisting motion around the PANI axis. In the UV-vis measurement, the  $\pi$ - $\pi^*$  transition absorption peak of PANI showed a blue shift by  $\beta$ -CD

inclusion. This means that this inclusion shortened  $\pi$ -conjugation of the PANI chain. Removal of the  $\pi$ - $\pi$  interaction and accompanying wide-angle twisting motion are probably the main factors for the blue shift.

#### 4. CONCLUSION

Molecular dynamics and its relation with the optical properties of PANI/ $\beta$ -CD IC were investigated using  $^{13}\text{C}$  spin-lattice relaxation measurements of solid state NMR and UV-vis absorption spectroscopies.  $\beta$ -CD inclusion accelerates twisting motion and increment of the twisting angle of the PANI chain, which is observed in an Arrhenius plot of the  $^{13}\text{C}$  spin-lattice relaxation rate, by removing tight  $\pi$ - $\pi$  stacking among intermolecular chains. These shorten the  $\pi$ -conjugation length, resulting in a blue-shift of the  $\pi$ - $\pi^*$  transition peak.

#### AUTHOR INFORMATION

##### Corresponding Author

\*E-mail: kyazawa@bio.titech.ac.jp.

#### ACKNOWLEDGMENTS

This work is supported by Urakami foundation. We would like to thank the Center of Advanced Materials Analysis for a kind help with the MALDI-TOF measurement.

#### REFERENCES

- (1) Chen, J.; Liu, Y.; Minett, A. I.; Lynam, C.; Wang, J.; Wallace, G. G. *Chem. Mater.* **2007**, *19*, 3595–3597.
- (2) Focke, W. W.; Wnek, G. E.; Wei, Y. J. *Phys. Chem.* **1987**, *91*, 5813–5818.
- (3) Macdiarmid, A. G.; Yang, L. S.; Huang, W. S.; Humphrey, B. D. *Synth. Met.* **1987**, *18*, 393–398.
- (4) Tanaka, H.; Gomez, M. A.; Tonelli, A. E.; Thakur, M. *Macromolecules* **1989**, *22*, 1208–1215.
- (5) Yazawa, K.; Inoue, Y.; Shimizu, T.; Tansho, M.; Asakawa, N. *J. Phys. Chem. B* **2010**, *114*, 1241–1248.
- (6) Obrzut, J.; Page, K. A. *Phys. Rev. B* **2009**, *80*, 195211.
- (7) Harada, A.; Li, J.; Kamachi, M. *Nature* **1993**, *364*, 516.
- (8) Harada, A.; Okada, M.; Li, J.; Kamachi, M. *Macromolecules* **1995**, *28*, 8406–8411.
- (9) Harada, A.; Suzuki, S.; Okada, M.; Kamachi, M. *Macromolecules* **1996**, *29*, 5611–5614.
- (10) Shuai, X.; Porbeni, F. E.; Wei, M.; Bullions, T.; Tonelli, A. E. *J. Mol. Struct.* **2003**, *650*, 175–180.
- (11) Yoshida, K.; Shimomura, T.; Ito, K.; Hayakawa, R. *Langmuir* **1999**, *15*, 910–913.
- (12) Shimomura, T.; Yoshida, K.; Ito, K.; Hayakawa, R. *Polym. Adv. Technol.* **2000**, *11*, 837.
- (13) Yuan, G.; Kuramoto, N.; Takeishi, M. *Polym. Adv. Technol.* **2003**, *14*, 428–432.
- (14) Grigoras, M.; Conduruta, D. G. *J. Inclusion Phenom. Macrocyclic Chem.* **2006**, *54*, 101.
- (15) Wang, B.; He, J.; Sun, D.; Zhang, R.; Han, B.; Huang, Y.; Yang, G. *Eur. Polym. J.* **2005**, *41*, 2483.
- (16) Sakuraba, H.; Hata, M.; Sato, K.; Tsuma, M. *Kobunshi Ronbunshu* **2006**, *63*, 331–340.
- (17) Belosludov, R. V.; Farajian, A. A.; Mizuseki, H.; Kawazoe, Y. *Comput. Mater. Sci.* **2006**, *36*, 130–134.
- (18) Lu, J.; Mirau, P. A.; Tonelli, A. E. *Macromolecules* **2001**, *34* (10), 3276–3284.
- (19) Girardeau, T. E.; Leisen, J.; Beckham, H. W. *Macromol. Chem. Phys.* **2005**, *206*, 998–1005.
- (20) Ceccato, M.; Nostro, P. L.; Rossi, C.; Bonechi, C.; Donati, A.; Baglioni, P. *J. Phys. Chem. B* **1997**, *101*, 5094–5099.
- (21) Dolan, A. D.; Wood, T. D. *J. Am. Soc. Mass Spectrom.* **2004**, *15*, 893–899.
- (22) Stejskal, E. O.; Schaefer, J.; Waugh, J. S. *J. Magn. Reson.* **1977**, *28*, 105.
- (23) Torchia, D. A. *J. Magn. Reson.* **1978**, *30*, 613.
- (24) Li, X.; Zhao, Y.; Zhuang, T.; Wang, G.; Gu, Q. *Colloids Surf., A* **2007**, *295*, 146–151.
- (25) Rusa, C. C.; Luca, C.; Tonelli, A. E. *Macromolecules* **2001**, *34*, 1318–1322.
- (26) Kim, Y. H.; Foster, C.; Chiang, J.; Heeger, A. J. *Synth. Met.* **1997**, *29*, 285–290.
- (27) Zhang, W. J.; Feng, J.; MacDiarmid, A. G.; Epstein, A. J. *Synth. Met.* **1997**, *84*, 119–120.
- (28) Gidley, M. J.; Bociek, S. M. *J. Am. Chem. Soc.* **1988**, *110*, 3820–3829.
- (29) Kaplan, S.; Conwell, E. M.; Richter, A. F.; MacDiarmid, A. G. *J. Am. Chem. Soc.* **1988**, *110*, 7647–7651.
- (30) Harada, A.; Li, J.; Kamachi, M. *Macromolecules* **1993**, *26*, 5698–5703.
- (31) Li, J.; Yan, D. *Macromol. Chem. Phys.* **2002**, *203*, 155–158.
- (32) Yazawa, K.; Inoue, Y.; Yamamoto, T.; Asakawa, N. *Phys. Rev. B* **2006**, *74*, 094204-1–094204-12.
- (33) Wei, Y.; Jang, G.; Hsueh, K. F.; Scherr, E. M.; MacDiarmid, A. G.; Epstein, A. J. *Polymer* **1992**, *33*, 314–322.